


**Vallejo, L.F., Rinas, U.**
**Folding and dimerization kinetics of bone morphogenetic protein-2, a member of the transforming growth factor-β family**
**(2013) FEBS Journal, 280 (1), pp. 83-92.**

# Folding and dimerization kinetics of bone morphogenetic protein-2, a member of the transforming growth factor-β family

Luis Felipe Vallejo[1] and Ursula Rinas[1,2]*

1 Helmholtz Centre for Infection Research, Braunschweig, Germany,

2 Leibniz University of Hannover, Technical Chemistry – Life Science, Hannover, Germany

*Corresponding author. Ursula.Rinas@helmholtz-hzi.de

## Abstract

The kinetic of folding and dimerization of bone morphogenetic protein-2 (BMP-2), a disulfide-connected, homodimeric cystine-knot protein and member of the transforming growth factor-β superfamily, was analyzed at a variety of different conditions. Refolding and dimerization of BMP-2 is a very slow process under all conditions studied which can be described by consecutive first-order reactions involving at least one long-lived intermediate. The rate constants vary from ~0.2 $10^{-5}$ to ~3.5 $10^{-5}$ $s^{-1}$ and are strongly dependent on temperature, redox conditions, and the presence of stabilizing or destabilizing ions. In particular, the combined impact of ionic strength and redox conditions on the rates indicates that electrostatic interactions are controlling thiol-disulfide exchange reactions on the path from the unfolded and reduced monomers to the disulfide-connected growth factor in a rate-determining way.

**Key words:** bone morphogenetic protein-2 (BMP-2), TGF-β family, cystine knot, protein folding and dimerization, kinetics

## Introduction

Bone morphogenetic protein-2 (BMP-2) is the most important growth factor employed for treatment of severe bone defects (e.g. long bone fracture non-unions, spinal surgeries, and oral maxillofacial surgeries) [1-4]. It is a homodimeric disulfide-bonded protein belonging to the transforming growth factor (TGF)-β family, a subgroup of the cystine-knot protein superfamily [5,6]. It shares with cystine-knot growth factors a similar monomer structure despite big differences in amino acid sequences [5,7] and with the TGF-β family also a remarkably similar dimer structure [6,8]. It is a naturally glycosylated protein but glycosylation it is not required for its function [9].

BMP-2 and other growth factors of the cystine-knot family are synthesized *in vivo* as large pre-pro-proteins [7]. The folded mature BMP-2 monomer contains 3 disulfide bonds which form the so-called cystine knot, an eight-member macrocycle in which two disulfide bonds participate and through which yet another disulfide bond is formed [8]. It has been proposed that the rigidity of the cystine-knot stabilizes the monomer as it lacks the common hydrophobic core of globular proteins [9]. In fact, there is experimental evidence that the cystine knot contributes significantly to the unusual high thermal stability of these proteins [10].

Dimerization of BMP-2 involves the formation of yet another disulfide bond which additionally stabilizes the protein [8]. BMP-2 can withstand strong denaturing conditions [11-13] even accompanied with high temperature treatments [14] and its inactivation requires the addition of reducing agents [13]. During dimerization two tightly packed hydrophobic cores are formed, however, large hydrophobic parts of the BMP-2 dimer are still exposed to the solvent contributing to its unusual low solubility in aqueous solutions [8,9].

BMP-2 is usually produced in its mature form by refolding from inclusion bodies of recombinant *E. coli* [15-17]. The prosequence does not contribute to efficient refolding [18],

but satisfactory refolding yields of the mature protein from solubilized inclusion body proteins are only obtained in the time scale of hours [15-17]. Despite it enormous importance in bone tissue engineering little is known on the rules controlling folding and dimerization of BMP-2 during renaturation.

Here, we describe for the first time the folding and dimerization kinetics of BMP-2 depending on protein concentration, temperature, redox conditions, and the presence of stabilizing or destabilizing additives. Our results show that under all conditions studied folding and dimerization is a very slow process involving at least one long-lived intermediate and follows first-order kinetics.

## Results

### BMP-2 folding and dimerization is a very slow process involving at least one long-lived intermediate and follows first-order kinetics

The kinetics of the formation of the disulfide-bonded BMP-2 dimer were analyzed in the absence or presence of sodium chloride at different initial concentrations of unfolded and reduced monomer. The time-dependent increase of the disulfide-bonded BMP-2 dimer, expressed as relative concentration in percentage of the initial amount of unfolded and reduced monomer, clearly followed a sigmoidal pattern indicating the presence of at least one long-lived intermediate on the folding and assembly pathway (Figure 1). Dimer formation was slower in the absence of sodium chloride, the sigmoidal shape more pronounced and, moreover, lower refolding yields were obtained (Figure 1). Under both conditions, however, the time-dependent increase of the BMP-2 dimer was independent on the initial concentration of the unfolded and reduced monomer indicating that the rate-limiting step during its formation was not governed by a second-order association step (Figure 1). A complete conversion of the reduced and unfolded monomer into the disulfide-bonded BMP-2 dimer was not achieved, thus, at least one misfolded monomerice BMP-2 end product is obtained during the refolding process.

Following, various kinetic models were analyzed which could describe the experimental data with sufficient accuracy. The simplest model with the best fitting to the experimental data included consecutive first-order reactions starting with the unfolded and reduced monomer leading to the correctly folded disulfide-bonded BMP-2 dimer and a first-order side reaction starting from a late pathway intermediate leading to misfolded monomeric BMP-2 (Figure 2A).

When BMP-2 refolding and dimerization studies were carried out under standard conditions without the addition of sodium chloride, at least two intermediates on the pathway from the reduced and unfolded monomer to the correctly folded BMP-2 dimer were required in the model to describe the experimental data with sufficient accuracy. Further addition of intermediates improved the fitting only marginally (Figure 2B). Furthermore, the fitting of the two-intermediate model to the experimental data was better when the first-order side reaction to the misfolded monomeric BMP-2 was assumed to occur from a late intermediate (e.g. $I_2$) rather than from the reduced and unfolded monomer (data not shown). Thus, refolding and dimerization of BMP-2 in the absence of sodium chloride is best described by a productive consecutive first-order reaction involving two intermediates and an unproductive side reaction diverting from the late intermediate.

When BMP-2 refolding and dimerization studies were performed under standard conditions in the presence of sodium chloride, the model could be further simplified. Under these conditions, only one intermediate was sufficient to adequately describe the experimental data (Figure 2C). For illustration, the fitting of a kinetic model assuming a second-order rate-limiting step to the experimental data is also shown (Figure 2C, insert). These results clearly demonstrate that the experimental data cannot be described by a kinetic model involving a second-order rate-determining dimerization step and prove that refolding and dimerization of BMP-2 clearly follow first-order kinetics.

## Constraints of the kinetic model

To facilitate a comparison of the folding and association kinetics at different conditions, kinetic constants should be determined employing the simplest kinetic model where adequate fitting to all experimental data is feasible. Thus, the model was reduced to a productive consecutive first-order reaction involving one intermediate and an unproductive first-order side reaction diverting from the intermediate. Accordingly, the concentrations of four different forms of BMP-2 (U, I, D, and X) and four kinetic constants ($k_u$, $k_i$, $k_d$, and $k_x$) are required to comprehensively describe the time-course of BMP-2 folding and dimerization. However, the different forms of BMP-2 are analytically not accessible. Only the initial concentration of the unfolded and reduced monomer and the time-dependent change in the concentration of the correctly folded and disulfide-bonded BMP-2 dimer can be accurately determined (for details refer to Doc1 in the supporting information). All other forms (U, I, X) cannot be discriminated as they are undistinguishable by non-reducing SDS-PAGE analysis. Thus, solving the corresponding mathematical equations yields several solutions compatible with the given data. Hence, restrictions were introduced into the mathematical model to limit the number of possible solutions (for details refer to Doc2 in the supporting information). With these restrictions the mathematical model could adequately describe the experimental time course data of BMP-2 folding and dimerization under a variety of different conditions, and thus was adopted in the following chapters.

## NaCl accelerates BMP-2 folding and dimerization and allows the process to take place at higher temperatures

The kinetics of folding and dimerization of BMP-2 were studied in standard refolding buffer with and without supplementation of NaCl (Figures 3 and 4). The experiments were performed at different temperatures ranging from zero up to 30°C.

The rate of folding and dimerization of BMP-2 as well as the final refolding yield increased strongly with increasing temperatures up to 15°C independent of the presence of NaCl (Figure 3A and B). Increasing the temperatures above 15°C strongly reduced the final refolding yield as well as the overall folding and dimerization rate of BMP-2 (Figure 3C and D). However, at all temperatures studied, the final refolding yield as well as the overall folding and dimerization rate of BMP-2 were higher when NaCl was added to the refolding buffer. Most importantly, refolding and dimerization of BMP-2 did not occur at temperatures above 25°C when NaCl was not added to the refolding buffer. However, refolding and dimerization of BMP-2 was still observed at 30°C when the refolding buffer was supplemented with NaCl.

A more detailed view on the refolding and dimerization of BMP-2 based on the model outlined in the previous section revealed that an increase in the refolding temperature up to 25°C resulted in an increase of the kinetic constant governing the formation of the intermediate ($k_u$) both in the absence or presence of NaCl (Figure 4A). However, the formation of the intermediate was generally faster when NaCl was added to the refolding buffer. The examination of the kinetic constant controlling the formation of the disulfide-bonded BMP-2 dimer ($k_d$) also revealed an increase with increasing temperature, but reached a maximum at different temperatures depending on the absence or presence of NaCl in the refolding buffer (Figure 4B). Without NaCl, the formation rate of the BMP-2 dimer already declined at temperatures above 15°C while the addition of NaCl shifted the maximal rate to 20°C. Above these temperatures a strong decline in the dimer formation rate ($k_d$) was observed. Furthermore, the kinetic constant governing the unproductive off-pathway reaction ($k_x$) increased with increasing temperatures but less pronounced when NaCl was added to the refolding buffer (Figure 4C). As a result of this dissimilar temperature dependence of the last on-pathway and the parallel off-pathway reaction originating from the intermediate, the final refolding yields increased only with temperature up to 15°C and declined at temperatures

above (Figure 4D). At all temperatures, folding and dimerization of BMP-2 in the presence of NaCl revealed higher rates for the productive on-pathway reactions, in particular for the last step on the path to the correct BMP-2 dimer ($k_d$). In contrast, the presence of NaCl caused a slight decrease in the rate of the unproductive off-pathway reaction ($k_x$). Thus, at all temperatures higher final refolding yields were achieved when NaCl was added to the refolding buffer. In particular, the large difference in the rate constants for the last on-pathway and the parallel off-pathway reaction at higher temperatures were responsible that the formation of the disulfide-bonded BMP-2 dimer was still observed at temperatures up to 30°C in the presence of NaCl while this temperature was reduced to 25°C in the absence of NaCl.

## Redox conditions strongly affect BMP-2 folding and dimerization

BMP-2 is a dimeric protein with seven cysteines per monomer which are all involved in distinct disulfide bonds (cystine knot and intermolecular disulfide bond), thus, redox conditions are expected to have an influence on BMP-2 folding and dimerization. Typically, a mixture of reduced and oxidized glutathione is employed to allow disulfide-bond forming and exchange reactions during renaturation of disulfide-bonded proteins [19]. Most often a strong excess of the reduced versus the oxidized glutathione (40:1) leads to the best renaturation yields.

Following, the ratio of glutathione reduced to glutathione oxidized was varied while the total concentration of glutathione was kept constant and the time-course of BMP-2 folding and dimerization (e.g. formation of the disulfide-bonded dimer) was studied. The overall folding and dimerization rate as well as the final refolding yield increased strongly when the redox environment was changed to more oxidizing conditions (Figures 5 and 6). However, at strongly oxidizing conditions the overall folding and dimerization slowed down concomitant with a strong decline in the refolding yield. A more detailed view revealed that an increase in the oxidizing conditions increased both the formation rate for the intermediate ($k_u$) as well as

for the misfolded off-pathway product ($k_x$) (Figure 6A and C) suggesting that both reactions are dominated by disulfide bond forming reactions. Interestingly, the formation rate for the disulfide-bonded dimer ($k_d$) exhibited a distinct maximum at intermediate redox conditions (Figure 6B) suggesting that this step is governed by the formation of (a) critical disulfide bond(s) requiring multiple reshuffling reactions for correct formation. As consequence, best refolding yields are also achieved at intermediate redox conditions (Figure 6D).

## Folding and dimerization of BMP-2 only slows down at guanidine chloride concentrations above 0.6 mol $L^{-1}$

The presence of the chaotropic agent Gdn-HC at low concentrations can effectively inhibit the aggregation of BMP-2 during renaturation [16]. Thus, the BMP-2 folding and dimerization kinetics were investigated at various Gdn-HCl concentrations. The overall rate of BMP-2 folding and dimerization was noticeably constant at Gdn-HCl concentrations below 0.6 mol $L^{-1}$ (Figure 7). However, at Gdn-HCl concentrations above 0.6 mol $L^{-1}$ the overall formation rate of the disulfide-bonded BMP-2 decreased considerably concomitant with a strong decline in the final refolding yield (Figures 7 and 8, respectively). The analysis of BMP-2 folding and dimerization based on the previously outlined model and depicted in form of so-called "chevron plots" (log $k_{obs}$ plotted vs denaturant concentration) for the individual reactions (Figure 8A-C) did not show a linear dependency of log $k_{obs}$ on the denaturant concentration as anticipated for two-state folding reactions. This finding clearly underlines that folding and dimerization of BMP-2 is more complex than represented in the outlined model. This model is sufficient to describe the experimental data under all conditions studied but does not necessarily depict the true pathway of folding and dimerization.

## Discussion

Refolding and dimerization of BMP-2 is an extremely slow process which does not depend on the protein concentration and can be described by consecutive first-order reactions involving at least one long-lived intermediate. Other dimeric cystine knot growth factors such as brain-derived neurotrophic factor [20], nerve growth factor [21,22], and platelet-derived growth factor (PDGF) [23] also exhibit slow folding and dimerization kinetics within time-scales of minutes and hours. However, refolding and dimerization of BMP-2 is even slower requiring hours up to days with rate constants ranging from ~0.2 $10^{-5}$ to ~3.5 $10^{-5}$ $s^{-1}$. The kinetics of folding and dimerization are strongly dependent on temperature, redox conditions, and the presence of stabilizing or destabilizing ions. Noteworthy is the accelerating effect of NaCl on the productive on-pathway reactions. As these reactions also depend on redox conditions, thus encompassing disulfide-forming and reshuffling reactions, the "NaCl effect" most likely reflects the influence of electrostatic interactions on the reactivity of cysteine thiols. For example, studies on peptides with sequence variations revealed that the local cysteine environment is important for thiol reactivity as it modifies electrostatic interactions between charged nearby side chains and the charged disulfide reagent [24,25]. And, moreover, these interactions are also responsive to variations in the ionic strength of the buffer (e.g. KCl concentration) which alter the reaction rate between peptide thiols and charged disulfide reagents such as oxidized glutathione [25].

Our results provide clear evidence that the association of two monomers, a second order reaction, does not have any important kinetic role, but that structural rearrangements, first-order reactions, are controlling the rate of BMP-2 folding and dimerization. However, our data do not give clear hints whether the last rate-determining step can be attributed to folding and disulfide-bond formation/reshuffling reactions at the monomer level or to (conformational) rearrangements of the dimerized protein not yet connected by an

intermolecular disulfide-bond. The latter might be more likely, since studies on the folding and dimerization of PDGF, also a cystine-knot protein and member of the transforming growth factor-β superfamily, revealed that structural rearrangements at the level of the dimerized but not yet disulfide-connected growth factor were rate-determining on the path from unfolded and reduced monomers to the disulfide-connected growth factor [23]. Following these rearrangements, the formation of intermolecular disulfide bonds between the PDGF chains was fast and kinetically irrelevant.

The results presented here shed first light on the kinetics of folding and dimerization of BMP-2 but also point to the need for more specific experimental data on the nature and time course of the various intermediates to get a thorough picture of this complex folding/dimerization process which involves the formation of intramolecular cystine knots as well as the formation of an intermolecular disulfide bond.

## Experimental procedures

### Production and purification of unfolded und reduced BMP-2 monomer

*E. coli* strain Rosetta™ (DE3) (Novagen, Madison, USA) hosting the temperature-inducible expression vector pCYTEXP3-BMP-2 was used to produce human BMP-2 in form of inclusion bodies [17]. Cells were grown in terrific broth (tryptone 12 g $L^{-1}$, yeast extract 24 g $L^{-1}$, glycerol 4 mL $L^{-1}$, $KH_2PO_4$ 2.3 g $L^{-1}$, and $K_2HPO_4$ 12.5 g $L^{-1}$) and inclusion bodies isolated as described previously [17]. All buffers were degassed rigorously with nitrogen prior to utilization. Inclusion bodies were first solubilized in 6 mol $L^{-1}$ guanidine hydrochloride (Gdn-HCl), 0.1 mol $L^{-1}$ Tris-HCl (pH 8.5), 1 mmol $L^{-1}$ EDTA, and 0.1 mol $L^{-1}$ dithiothreitol (DTT). After overnight incubation at 20°C, DTT removal was accomplished by dialysis against 6 mol $L^{-1}$ Gnd-HCl, 50 mmol $L^{-1}$ 2-[N-morpholino]-ethanesulfonic acid (pH 5.0), and 1 mmol $L^{-1}$ EDTA (residual DTT concentration after dialysis < 1 mmol $L^{-1}$). This solution containing the unfolded and reduced BMP-2 monomer (14 mg $mL^{-1}$) was stored in aliquots at -70°C and thawed directly prior to the refolding experiment. Protein concentration was determined using a bicinchoninic acid assay following manufacturer's instructions (Pierce, USA). In addition, BMP-2 concentration and purity was verified by SDS-PAGE performed under reducing conditions using precast 8-16% gels (Criterion, Biorad, Hercules, USA). Quantification was done by densitometry of Coomassie-Brilliant-Blue-stained gels using purified and refolded BMP-2 as standard [17]. The protein concentration of the standard was determined by UV280 using a molar extinction coefficient of 18860 L $mol^{-1}$ $cm^{-1}$ which was calculated as described previously [26]. The standard was treated with 0.1 mol $L^{-1}$ DTT prior to electrophoresis. The concentration of unfolded and reduced BMP-2 monomer determined by the two methods adequately agreed.

## Refolding and dimerization studies

Standard refolding and dimerization conditions were as follows: unfolded and reduced BMP-2 monomer (purity > 95%) was diluted to a final concentration of 0.1 mg $mL^{-1}$ in a renaturation buffer containing (final concentrations) 0.5 mol $L^{-1}$ Gnd-HCl, 0.1 mol $L^{-1}$ Tris-HCl (pH 8.5), 0.75 mol $L^{-1}$ 2-(cyclohexylamino)ethanesulfonic acid (CHES), 5 mmol $L^{-1}$ EDTA, and 3 mmol $L^{-1}$ total glutathione in a 2:1 ratio of glutathione reduced to glutathione oxidized (GSH:GSSG) and incubated at 10°C to allow BMP-2 refolding and dimerization. All buffers were degassed rigorously with nitrogen prior to utilization. Samples from the refolding mixture were treated immediately with 0.1 mol $L^{-1}$ iodoacetate (final concentration) to prevent further disulfide bond formation and scrambling prior to electrophoresis under non-reducing conditions using precast 8-16% SDS-PAGE gels. After Coomassie-Brilliant-Blue staining, the disulfide-bonded BMP-2 dimer was quantified by densitometry using known concentrations of pure refolded and dimerized BMP-2 as standard. Correct folding and dimerization of BMP-2 was verified through its binding to the extracellular ligand-binding domain of the BMP-receptor type IA [27]. Aggregation was not observed under all conditions studied. For more details refer to Doc1 in the supporting information.

## Mathematical fitting of experimental data

The reactions used to describe the refolding and dimerization process were as follows,

$$\frac{dX}{dt} = \sum_{1}^{m} k_i Y_{ei}^{\,n_i} - \sum_{1}^{p} k_i Y_i^{\,n_i} \qquad (1)$$

where $Y_{ei}$ represents the reactant of all reactions in which the component $Y_i$ is formed. The second term of the equation represents all reactions in which $Y_i$ acts as a reactant. The kinetic constants are represented by $k_i$ and the reaction order of the respective reaction by $n_i$. The differential equations were simultaneously solved to fit the experimental data (Simulink, The

Mathworks, Natick, MA, USA). Experimental input data consisted of the time dependent concentrations of the correctly folded and disulfide-bonded BMP-2 dimer and initial concentrations of unfolded and reduced BMP-2 monomer.

## Acknowledgements

We are grateful to Volker Hecht for fruitful suggestions concerning the mathematical model.

## References


1 Cancedda R, Giannoni P, & Mastrogiacomo M (2007) A tissue engineering approach to bone repair in large animal models and in clinical practice. *Biomaterials* **28,** 4240-4250.

2 Bessa PC, Casal M, & Reis RL (2008) Bone morphogenetic proteins in tissue engineering: the road from the laboratory to the clinic, part I (basic concepts). *J Tissue Eng Regen Med* **2,** 1-13.

3 Bessa PC, Casal M, & Reis RL (2008) Bone morphogenetic proteins in tissue engineering: the road from laboratory to clinic, part II (BMP delivery). *J Tissue Eng Regen Med* **2,** 81-96.

4 Lo KW, Ulery BD, Ashe KM, & Laurencin CT (2012) Studies of bone morphogenetic protein based surgical repair. *Adv Drug Deliv Rev* in press.

5 Isaacs NW (1995) Cystine knots. *Curr Opin Struct Biol* **5,** 391-395.

6 Griffith DL, Keck PC, Sampath TK, Rueger D, & Carlson WD (1996) Three dimensional structure of recombinant human osteogenic protein 1; structural paradigm for the transforming growth factor β superfamily. *Proc Natl Acad Sci USA* **93,** 878-883.

7 McDonald NQ & Hendrickson WA (1993) A structural superfamily of growth factors containing a cystine knot motif. *Cell* **73,** 421-424.

8 Scheufler C, Sebald W, & Hülsmeyer M (1999) Crystal structure of human bone morphogenetic protein-2 at 2.7 Å resolution. *J Mol Biol* **287,** 103-115.

9 Ruppert R, Hoffmann E, & Sebald W (1996) Human bone morphogenetic protein 2 contains a heparin-binding site which modifies its biological activity. *Eur J Biochem* **237,** 295-302.

10 Muller YA, Heiring C, Misselwitz R, Welfle K, & Welfle H (2002) The cystine knot promotes folding and not thermodynamic stability in vascular endothelial growth factor. *J Biol Chem* **277,** 43410-43416.

11 Bessho K, Kusumoto K, Fujimura K, Konishi Y, Ogawa Y, Tani Y, & Iizuka T (1999) Comparison of recombinant and purified human bone morphogenetic protein. *Br J Oral Maxillofac Surg* **37,** 2-5.

12 Wang EA, Rosen V, Cordes P, Hewick RM, Kriz MJ, Luxenberg DP, Sibley BS, & Wozney JM (1988) Purification and characterization of other distinct bone-inducing factors. *Proc Natl Acad Sci U S A* **85,** 9484-9488.

13 Sampath TK & Reddi AH (1981) Dissociative extraction and reconstitution of extracellular matrix components involved in local bone differentiation. *Proc Natl Acad Sci U S A* **78,** 7599-7603.

14 Sato T, Iwata H, Takahashi M, & Miura T (1993) Heat tolerance of activity toward ectopic bone formation by rabbit bone matrix protein. *Ann Chir Gynaecol Suppl* **207,** 37-40.

15 von Einem S, Schwarz E, & Rudolph R (2010) A novel TWO-STEP renaturation procedure for efficient production of recombinant BMP-2. *Protein Expr Purif* **73,** 65-69.

16 Vallejo LF & Rinas U (2004) Optimized procedure for renaturation of recombinant human bone morphogenetic protein-2 at high protein concentration. *Biotechnol Bioeng* **85,** 601-609.

17 Vallejo LF, Brokelmann M, Marten S, Trappe S, Cabrera-Crespo J, Hoffmann A, Gross G, Weich HA, & Rinas U (2002) Renaturation and purification of bone morphogenetic protein-2 produced as inclusion bodies in high-cell-density cultures of recombinant *Escherichia coli*. *J Biotechnol* **94,** 185-194.

18 Hillger F, Herr G, Rudolph R, & Schwarz E (2005) Biophysical comparison of BMP-2, proBMP-2 and the free propeptide reveals stabilization of the pro-peptide by the mature growth factor. *J Biol Chem* **250,** 14974-14980.

19 Vallejo LF & Rinas U (2004) Strategies for the recovery of active proteins through refolding of bacterial inclusion body proteins. *Microb Cell Fact* **3,** 11.

20 Philo JS, Rosenfeld R, Arakawa T, Wen J, & Narhi LO (1993) Refolding of brain-derived neurotrophic factor from guanidine hydrochloride: kinetic trapping in a collapsed form which is incompetent for dimerization. *Biochemistry* **32,** 10812-10818.

21 Rattenholl A, Lilie H, Grossmann A, Stern A, Schwarz E, & Rudolph R (2001) The pro-sequence facilitates folding of human nerve growth factor from *Escherichia coli* inclusion bodies. *Eur J Biochem* **268,** 3296-3303.

22 Rattenholl A, Ruoppolo M, Flagiello A, Monti M, Vinci F, Marino G, Lilie H, Schwarz E, & Rudolph R (2001) Pro-sequence assisted folding and disulfide bond formation of human nerve growth factor. *J Mol Biol* **305,** 523-533.

23 Müller C, Richter S, & Rinas U (2003) Kinetics control preferential heterodimer formation of platelet-derived growth factor from unfolded A- and B-chains. *J Biol Chem* **278,** 18330-18335.

24 Wu C, Belenda C, Leroux JC, & Gauthier MA (2011) Interplay of chemical microenvironment and redox environment on thiol-disulfide exchange kinetics. *Chem Eur J* **17,** 10064-10070.

25 Bulaj G, Kortemme T, & Goldenberg DP (1998) Ionization-reactivity relationships for cysteine thiols in polypeptides. *Biochemistry* **37,** 8965-8972.

26 Wetlaufer DB (1962) Ultraviolet spectra of proteins and amino acids. *Adv Prot Chem* **17,** 303-390.

27 Wendler J, Vallejo LF, Rinas U, & Bilitewski U (2005) Application of an SPR-based receptor assay for the determination of biologically active recombinant bone morphogenetic protein-2. *Anal Bioanal Chem* **381,** 1056-1064.

## Figure captions

**Figure 1** Folding and dimerization of BMP-2 at different protein concentrations.

Folding and dimerization of BMP-2 was studied at different initial concentrations of unfolded and reduced BMP-2 monomers and experiments carried out at 10°C in standard refolding buffer (**A**) and standard refolding buffer supplemented with 1 mol $L^{-1}$ NaCl (**B**). The time-dependent increase of dimeric disulfide-bonded BMP-2 is shown in relative concentrations as refolding yield. Initial concentrations of unfolded and reduced BMP-2 monomers (in μmol $L^{-1}$): 3.85 (○), 7.7 (◁), 11.5 (△), 15.4 (▽), 19.5 (▷), and 23.1 (□).

**Figure 2** Kinetic model of BMP-2 folding and dimerization.

Reactions describing the folding and dimerization of BMP-2 starting from unfolded and reduced monomers, U, passing through n intermediates, $I_n$, and finally, leading to the correctly folded, disulfide-connected dimeric BMP-2, D. An unproductive side reaction leads to misfoded monomeric BMP-2, X (**A**). Model-based description of the kinetics of folding and dimerization of BMP-2 in standard refolding buffer (**B**) and standard refolding buffer supplemented with 1 mol $L^{-1}$ NaCl (**C**) at different initial concentrations of unfolded and reduced BMP-2 monomers. The time-dependent increase of dimeric disulfide-bonded BMP-2 is shown in relative concentrations as refolding yield. Experimental data and conditions as described in Figure 1. (**B**): The best fitting of the model to the experimental data (absence of NaCL) assuming consecutive first-order reactions with 1 (solid line), 2 (dashed line), and 3 intermediates (dotted line). Appropriate fitting is obtained with 2 intermediates and the following first-order rate constants: $k_u$= 1.00 * $10^{-5}$ $s^{-1}$, $k_{i1}$= 0.98 * $10^{-5}$ $s^{-1}$, $k_d$= 0.55 * $10^{-5}$ $s^{-1}$, $k_x$= 0.44 * $10^{-5}$ $s^{-1}$. The insert depicts the first hours in more detail. (**C**): The best fitting of the model to the experimental data (presence of NaCl) assuming consecutive first-order reactions with one intermediate and the following first-order rate constants: $k_u$= 0.49 * $10^{-5}$ $s^{-1}$, $k_d$= 0.98 * $10^{-5}$ $s^{-1}$, $k_x$= 0.658 *$10^{-5}$ $s^{-1}$. The insert depicts the best fitting assuming a second-order dimerization step with the following rate rate constants: $k_u$= 0.31 * $10^{-5}$ $s^{-1}$, $k_d$= 1.30 * $10^{-5}$ $mol^{-1}$ L $s^{-1}$, $k_x$= 0.75 * $10^{-5}$ $s^{-1}$ (initial concentration of unfolded and reduced monomers in µmol $L^{-1}$: 3.85 (solid line), 7.7 (dashed line), 19.5 (dotted line), 23.1 (dashed-dotted line).

**Figure 3** Effect of temperature on the kinetics of BMP-2 folding and dimerization.

Folding and dimerization of BMP-2 was studied at different temperatures ranging from 0°C – 15°C (**A and B**) and from 15°C – 30°C (**C and D**) in standard refolding buffer (**A and C**) and standard refolding buffer supplemented with 1 mol $L^{-1}$ NaCl (**B and D**). Initial concentration of reduced and unfolded monomer was 0.1 mg $mL^{-1}$ (7.7 µmol $L^{-1}$). Fitting curves were obtained considering consecutive first-order reactions with one intermediate and rate constants as depicted in Figure 4. Temperature in °C: 0 (□), 5 (○), 10 (△), 15 (▽), 20 (◇), 25 (◁), and 30 (▷).

**Figure 4** Temperature dependence of rate constants and final refolding yields.

Influence of temperature on the different rate constants governing the productive consecutive first-order reactions (**A and B**) and the unproductive off-pathway reaction (**C**) and the final refolding yield (**D**). Folding and dimerization was followed in standard refolding buffer (○) and standard refolding buffer supplemented with 1 mol $L^{-1}$ NaCl (□). Kinetics constants were obtained after best fitting of the experimental data (Figure 3) using the simplified model involving one intermediate. For details of the model constraints please refer to Doc2 in the supporting information. Standard deviations of two different experiments are shown as error bars.

**Figure 5** Effect of redox condtions on the kinetics of BMP-2 folding and dimerization. Folding and dimerization of BMP-2 was studied at different redox conditions at 20°C in standard refolding buffer supplemented with 1 mol $L^{-1}$ NaCl. Initial concentration of reduced and unfolded monomer was 0.1 mg $mL^{-1}$ (7.7 µmol $L^{-1}$). Fitting curves were obtained considering consecutive first-order reactions with one intermediate and rate constants as depicted in Figure 6. The redox conditions were varied while the total glutathione concentration was kept at 3 mmol $L^{-1}$: GSH:GSSG: 1:5 (□), 2:1 (○), 10:1 (△), 20:1 (▽), and 40:1 (◇).

**Figure 6** Redox condition dependence of rate constants and final refolding yields. Influence of redox conditions on the different rate constants governing the productive consecutive first-order reactions (**A and B**) and the unproductive off-pathway reaction (**C**) and the final refolding yield (**D**). Folding and dimerization was followed at different GSH:GSSH ratios (3 mmol $L^{-1}$ total glutathione) at 20°C in standard refolding buffer supplemented with 1 mol $L^{-1}$ NaCl. Kinetic constants were obtained after best fitting of the experimental data (Figure 5) using the simplified model involving one intermediate. For details of the model constraints please refer to Doc2 in the supporting information. Standard deviations of two different experiments are shown as error bars.

**Figure 7** Effect of ionic denaturant concentration on the kinetics of BMP-2 folding and dimerization.

Folding and dimerization of BMP-2 was studied at different concentrations of Gdn-HCl at 10°C in standard refolding buffer. Initial concentration of reduced and unfolded monomer was 0.1 mg $mL^{-1}$ (7.7 µmol $L^{-1}$). Fitting curves were obtained considering consecutive first-order reactions with one intermediate and rate constants as depicted in Figure 8. Concentration of Gdn-HCl in mol $L^{-1}$: 0.3 (□), 0.4 (△), 0.5 (▽), 0.6 (○), 0.7 (■), 0.77 (▲), and 0.85 (●).

**Figure 8** Ionic denaturant concentration dependence of rate constants and final refolding yields.

Influence of ionic denaturant concentration on the different rate constants governing the productive consecutive first-order reactions (**A and B**) and the unproductive off-pathway reaction (**C**) and the final refolding yield (**D**). Folding and dimerization was followed at different Gdn-HCl concentrations at 10°C in standard refolding buffer. Kinetics constants were obtained after best fitting of the experimental data (Figure 7) using the simplified model involving one intermediate and depicted in so-called "Chevron plots". For details of the model constraints please refer to Doc2 in the supporting information. Standard deviations of two different experiments are shown as error bars.

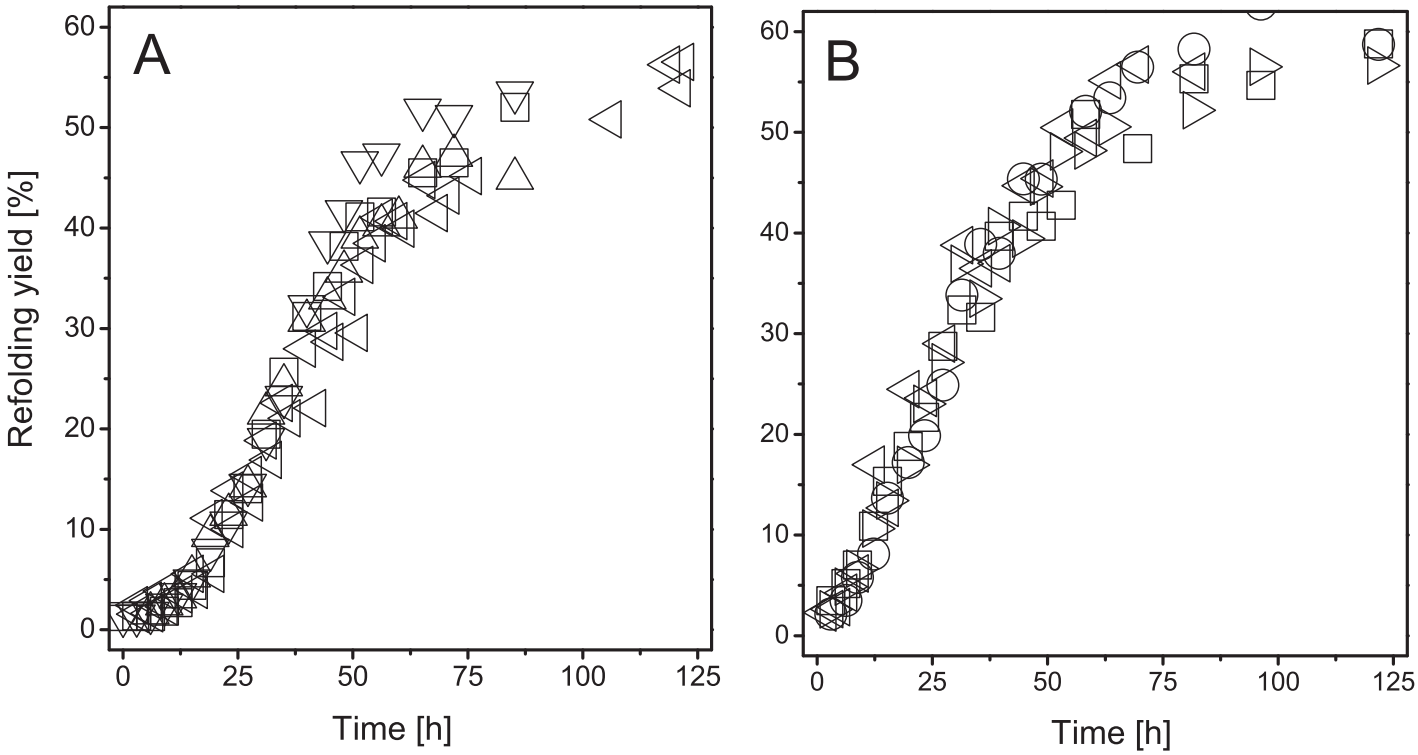
A
B
Refolding yield [%]
Time [h]
Time [h]
0
10
20
30
40
50
60
0
25
50
75
100
125

Figure 1

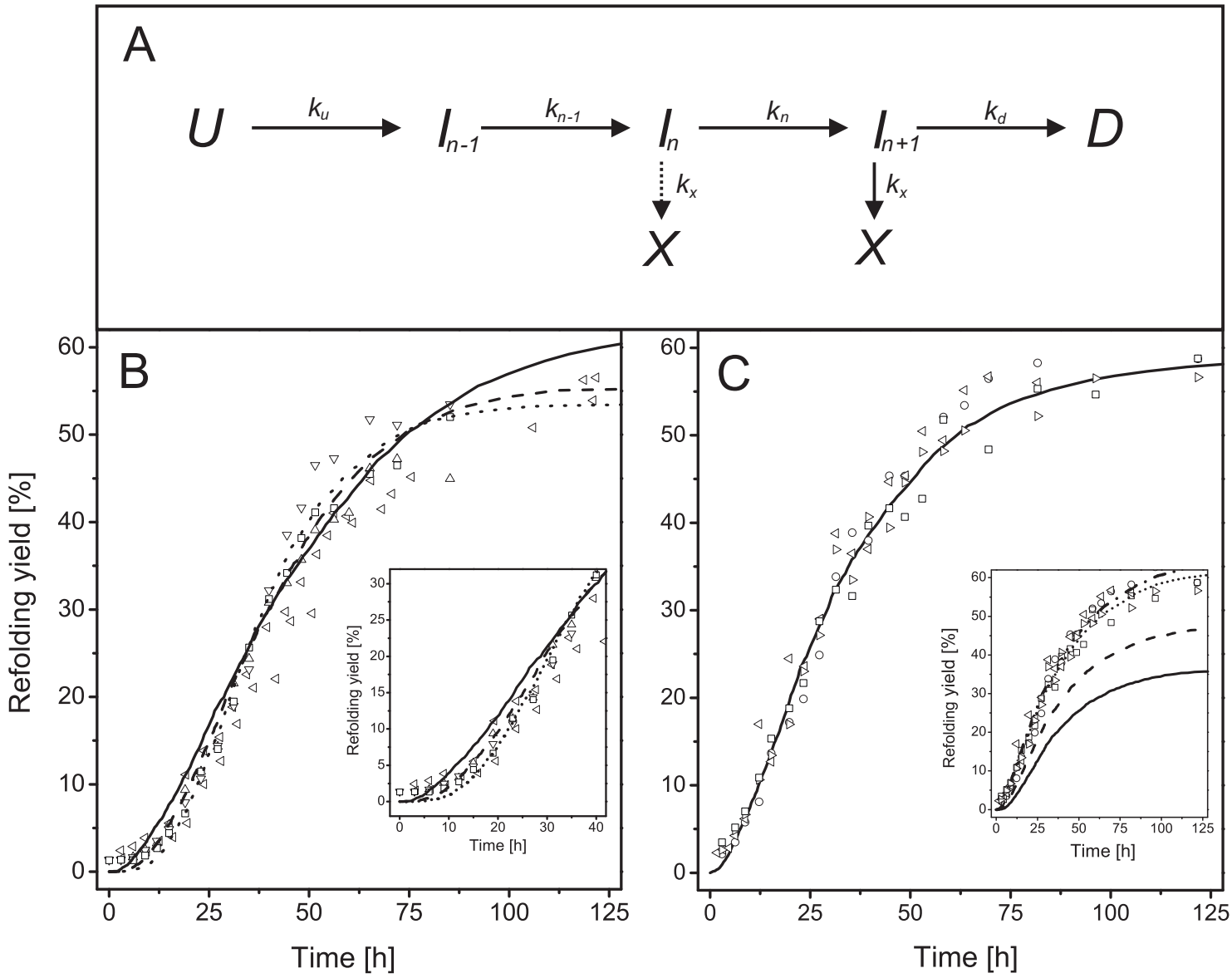
A
U
$k_u$
$I_{n-1}$
$k_{n-1}$
$I_n$
$k_n$
$I_{n+1}$
$k_d$
D
$k_x$
X
$k_x$
X
B
C
Refolding yield [%]
Time [h]
Refolding yield [%]
Time [h]
Refolding yield [%]
Time [h]

Figure 2

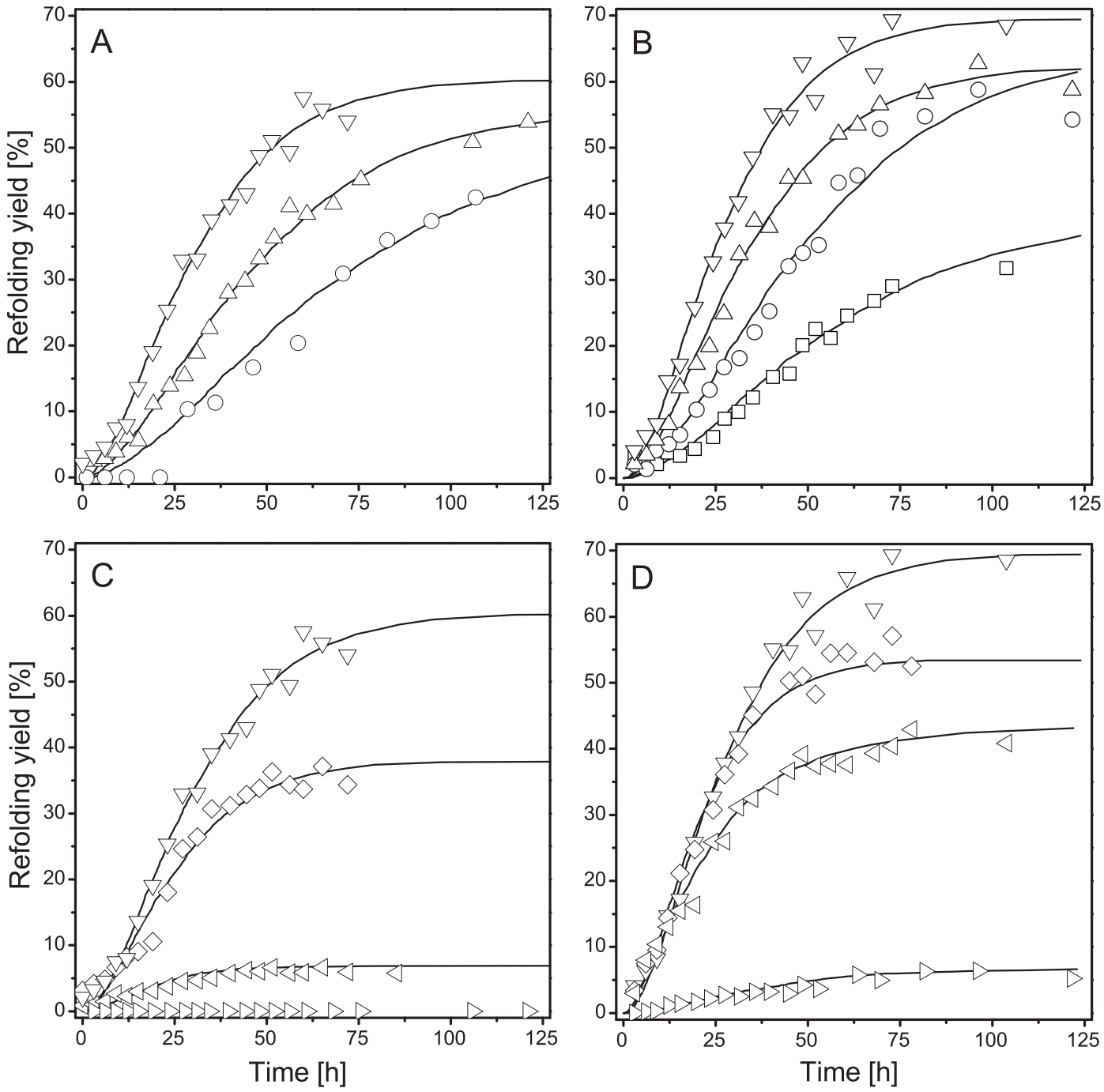
A
B
C
D
Refolding yield [%]
Time [h]
0
10
20
30
40
50
60
70
0
25
50
75
100
125

Figure 3

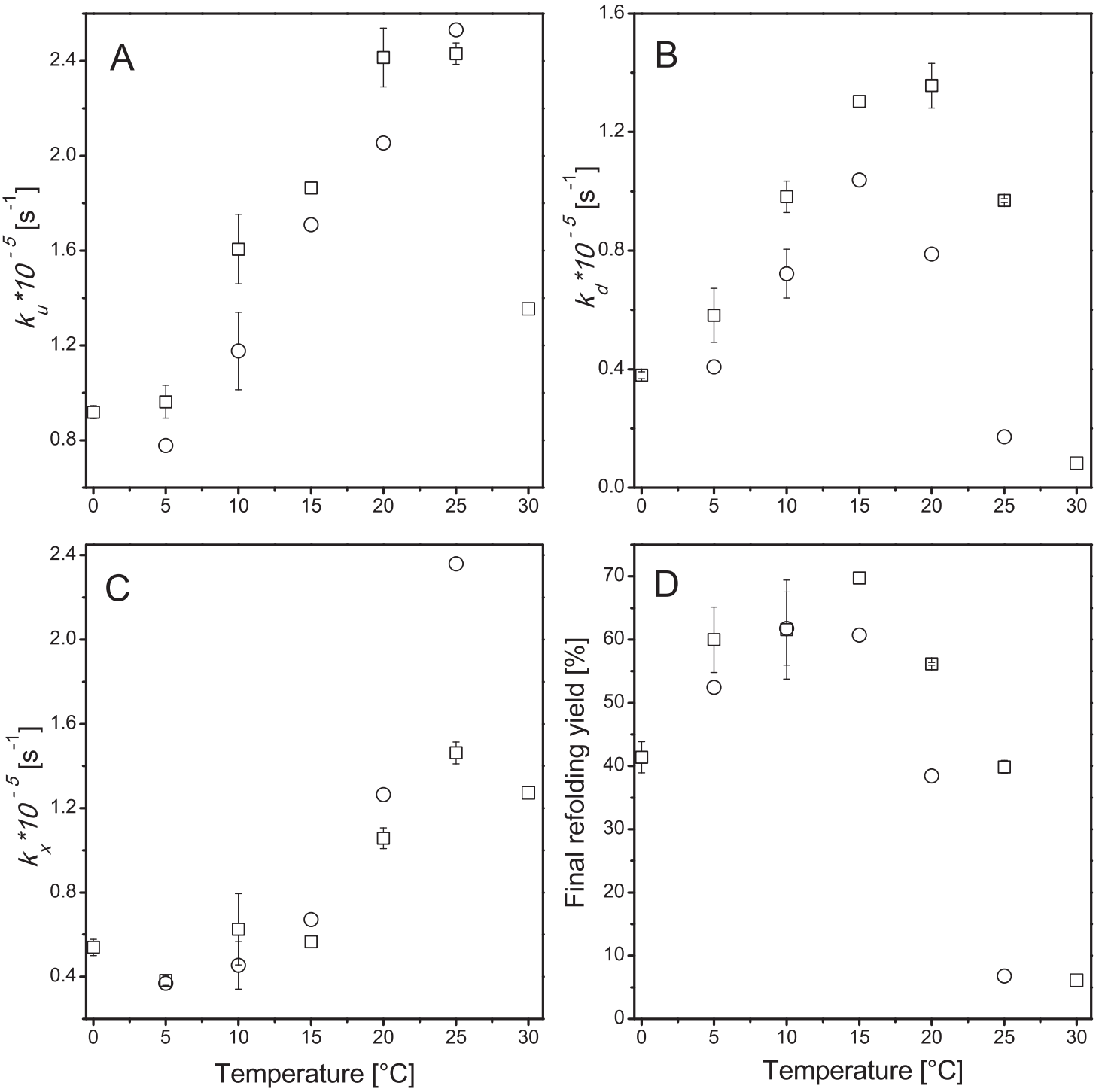
A
B
C
D
$k_u * 10^{-5}$ [s$^{-1}$]
$k_d * 10^{-5}$ [s$^{-1}$]
$k_x * 10^{-5}$ [s$^{-1}$]
Final refolding yield [%]
Temperature [°C]
Temperature [°C]

Figure 4

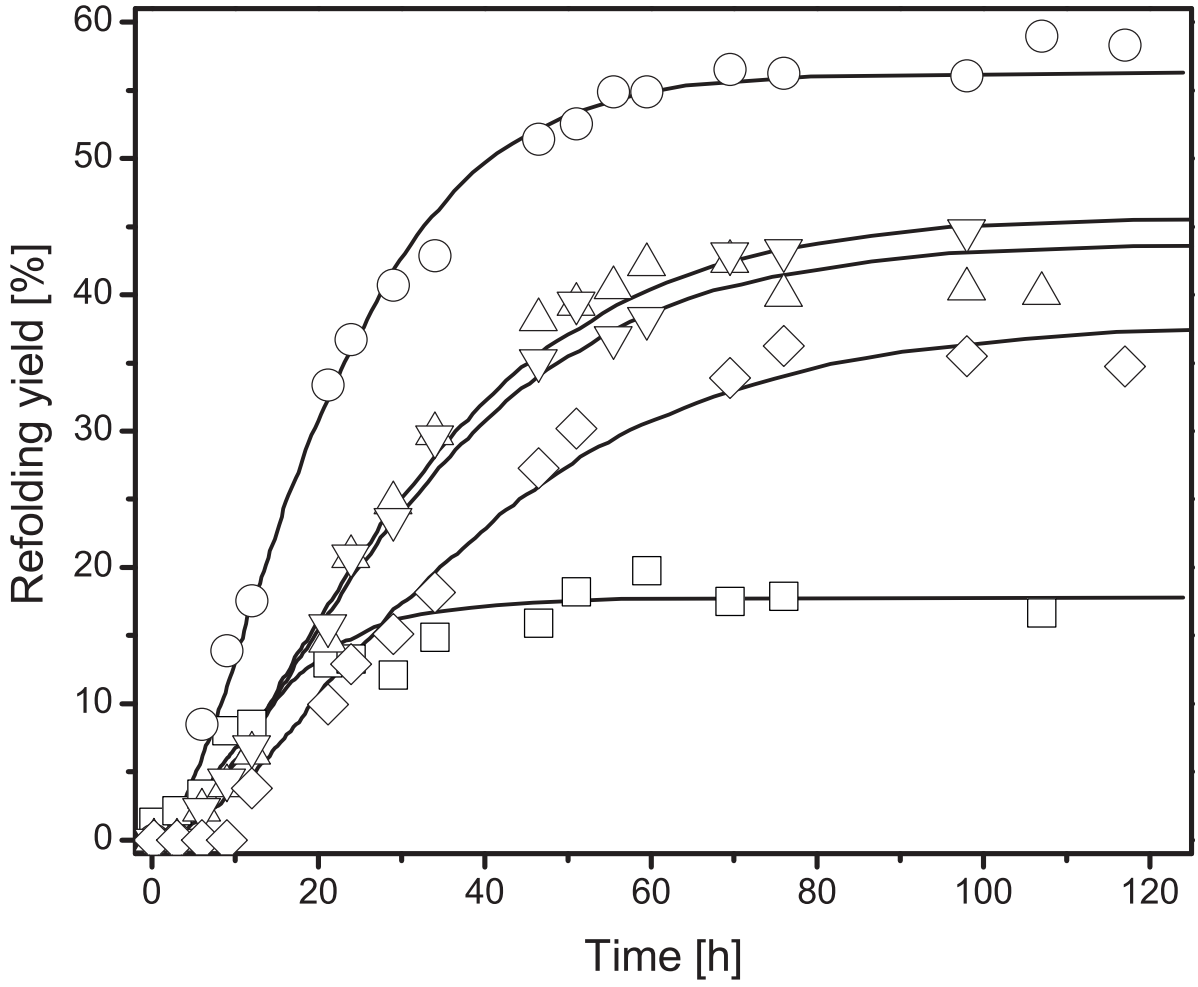


Figure 5

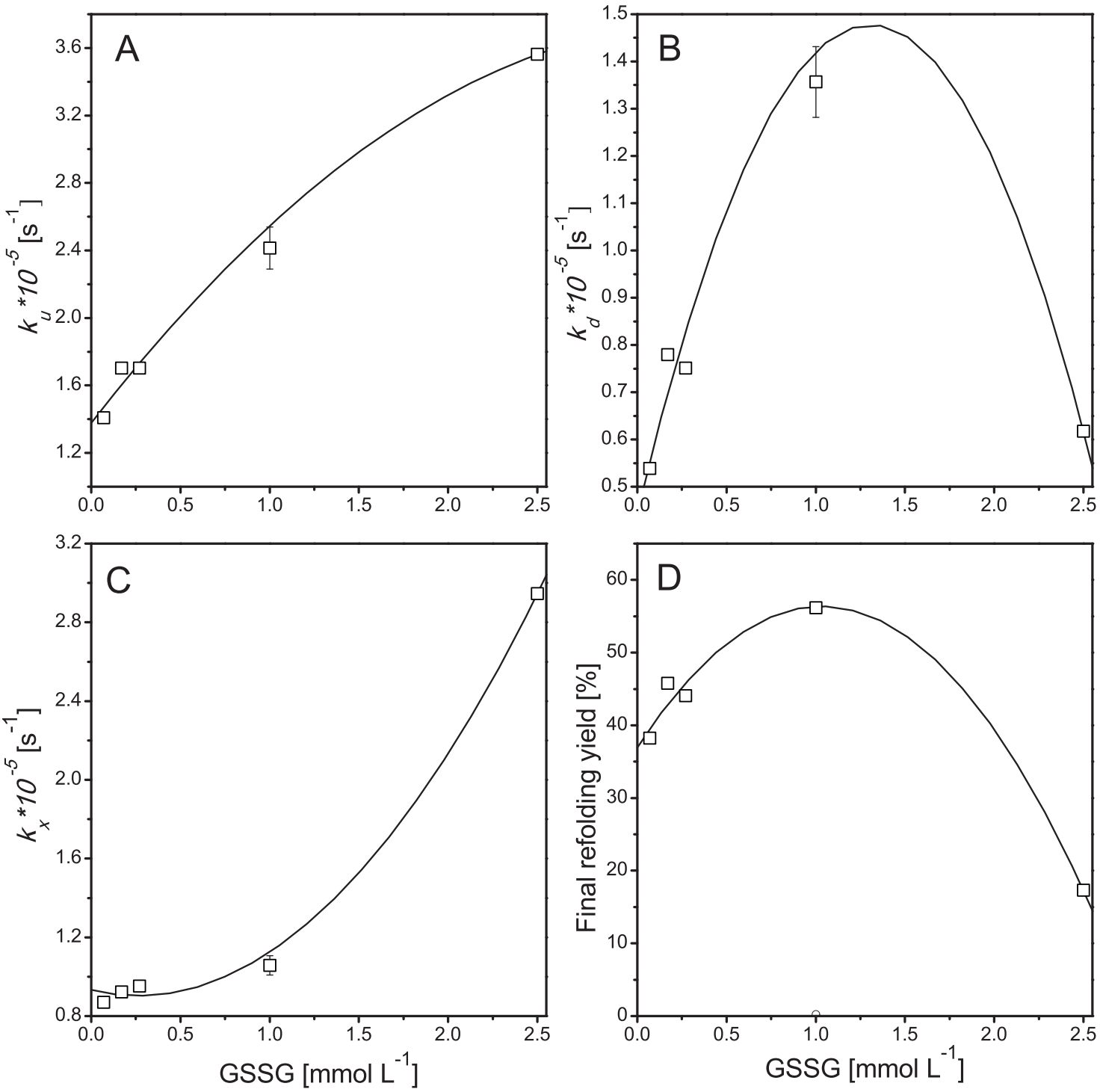
A
B
C
D
$k_u *10^{-5}$ [s$^{-1}$]
$k_d *10^{-5}$ [s$^{-1}$]
$k_x *10^{-5}$ [s$^{-1}$]
Final refolding yield [%]
GSSG [mmol L$^{-1}$]
GSSG [mmol L$^{-1}$]

Figure 6

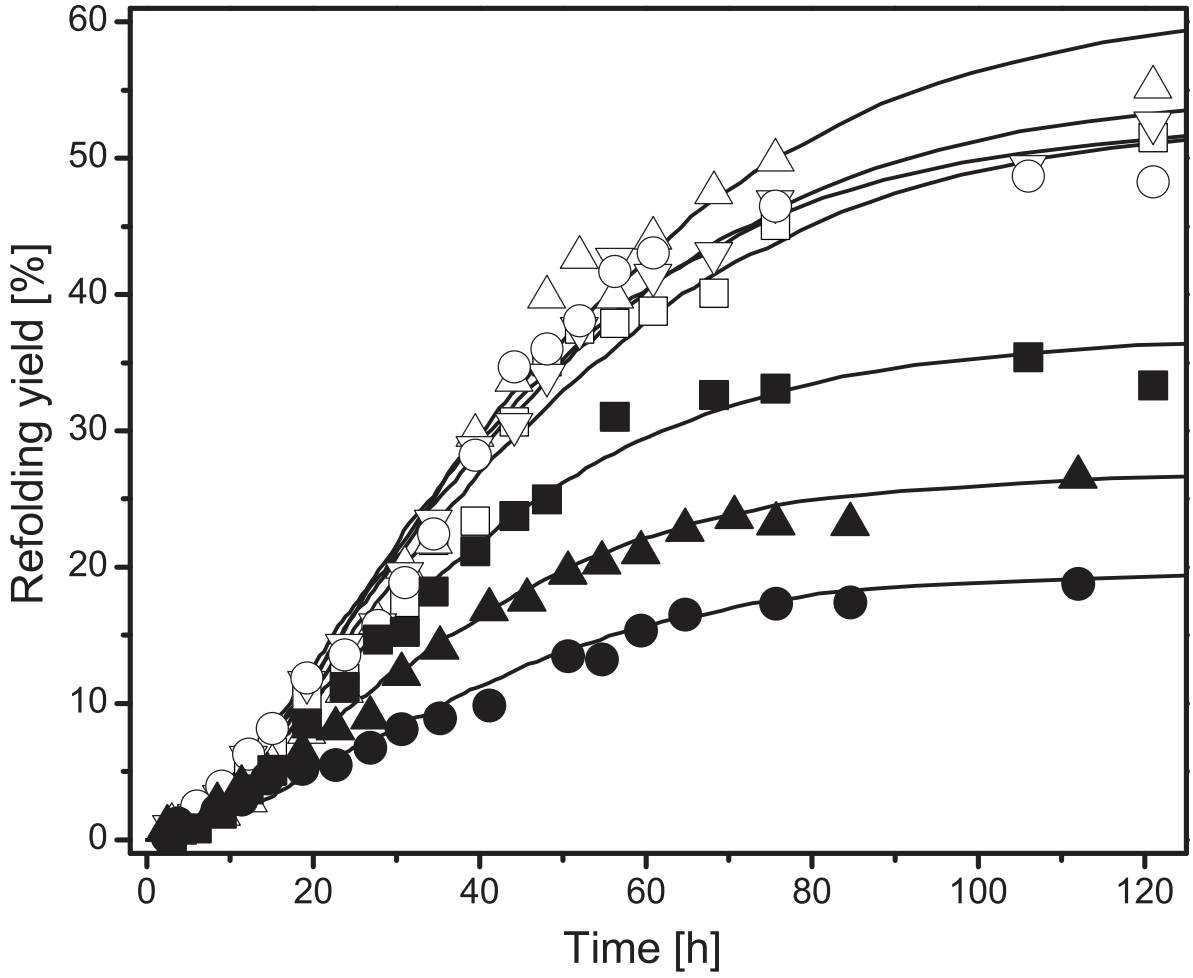


Figure 7

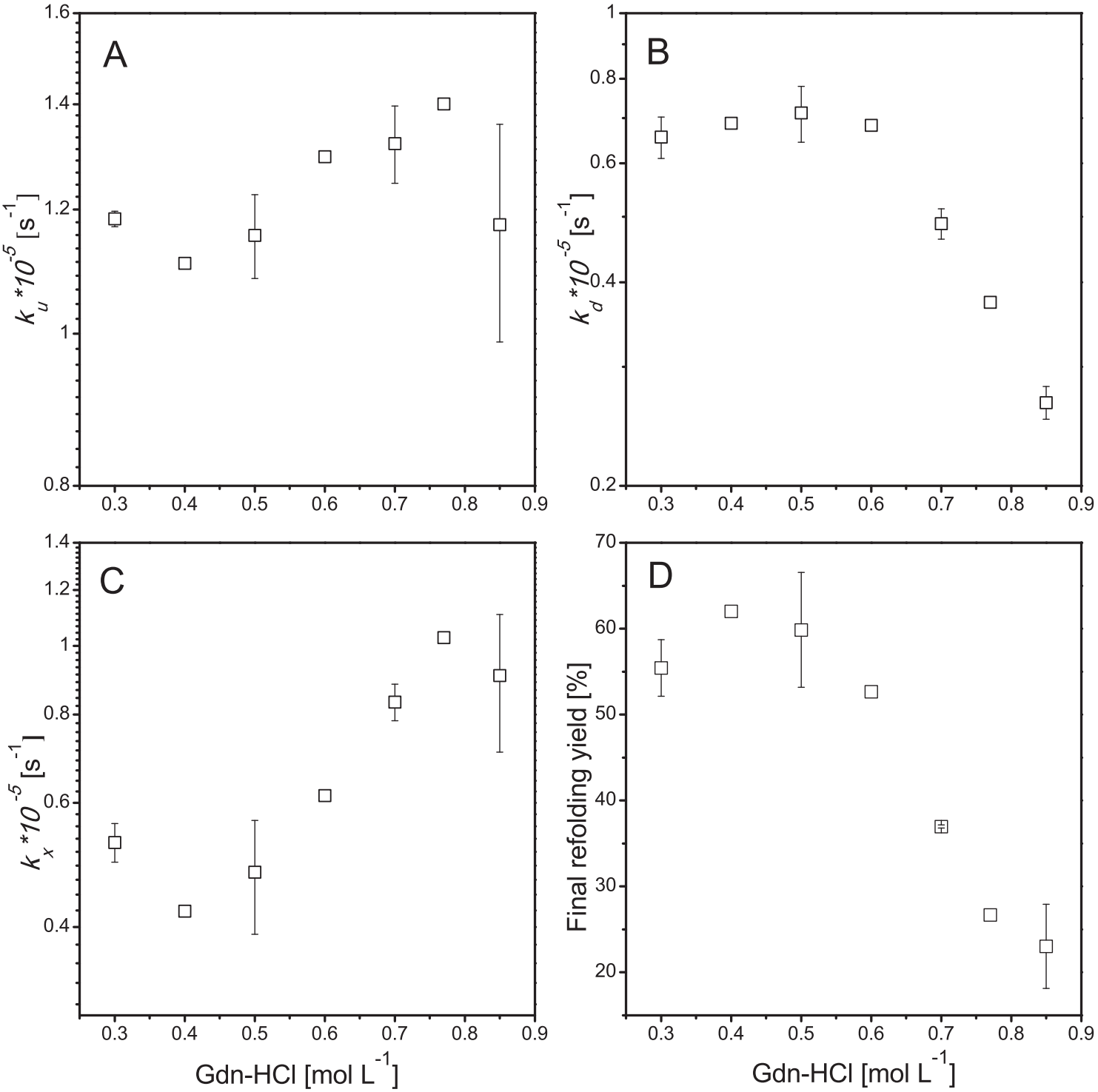
A
B
C
D
$k_u * 10^{-5}$ [s$^{-1}$]
$k_d * 10^{-5}$ [s$^{-1}$]
$k_x * 10^{-5}$ [s$^{-1}$]
Final refolding yield [%]
Gdn-HCl [mol L$^{-1}$]
Gdn-HCl [mol L$^{-1}$]

Figure 8

Supporting information to

# Folding and dimerization kinetics of bone morphogenetic protein-2, a member of the transforming growth factor-β family

Luis Felipe Vallejo[1] and Ursula Rinas[1,2]*

1 Helmholtz Centre for Infection Research, Braunschweig, Germany

2 Leibniz University of Hannover, Technical Chemistry – Life Science, Hannover, Germany

*Corresponding author. Ursula.Rinas@helmholtz-hzi.de

## Doc1 – Experimental analysis of folding and dimerization

Samples from the refolding experiment were subjected to non-reducing SDS-PAGE analysis as described in the Experimental procedures. The time-dependent increase of the disulfide-bonded dimeric BMP-2 (denoted D in Suppl. Fig 1A) was determined by densitometry, and it was, except for the initial concentration of the unfolded and reduced monomer, the only variable for which quantitative data were accessible in sufficient accuracy (Suppl. Fig. 1). These data were used for modeling purposes. The time-dependent change in the concentration of BMP-2 variants running at the monomer position (denoted M in Suppl. Fig 1A) under non-reducing concentrations were not considered for modeling as they represent different folding as well as misfolding variants/intermediates containing intermediary disulfide bonds. Moreover, a dimerized BMP-2 not yet connected by an intermolecular disulfide-bond would also run at the position of the monomer under non-reducing conditions. For the dimerized disulfide-bonded BMP-2 it was shown that it is biologically active i.e. is able to bind to the extracellular ligand-binding domain (ECD) of the BMP receptor type 1A with high affinity. A detailed description of the assay conditions to follow the formation of the disulfide-bonded BMP-2 dimer during refolding experiments by binding to the ECD of the BMP-receptor type IA, tagged with the Fc part of IgG (BMPR-IA-Fc) using an optical biosensor system (Biacore 2000, Biacore AB, Uppsala, Sweden) is given elsewhere (Wendler et al., 2005).

Wendler J, Vallejo LF, Rinas U, & Bilitewski U (2005) Application of an SPR-based receptor assay for the determination of biologically active recombinant bone morphogenetic protein-2. Anal Bioanal Chem 381, 1056.

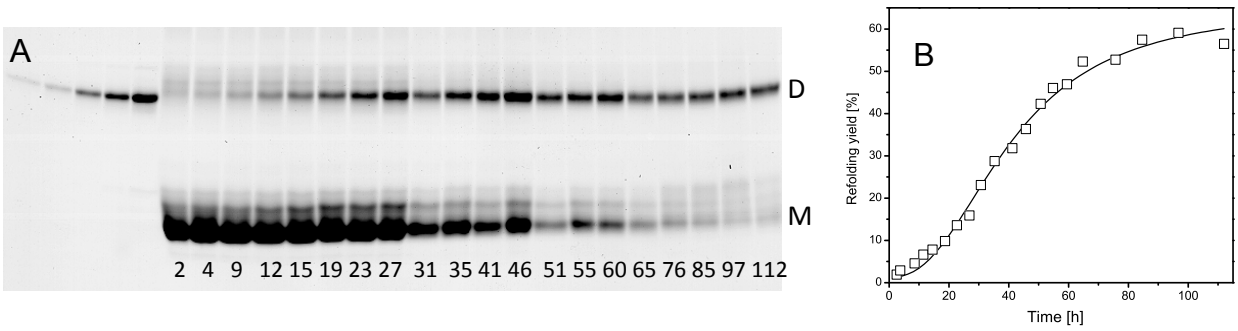


**Suppl Figure 1** Analysis of the kinetics of the formation of the disulfide-bonded BMP-2 dimer from unfolded and reduced BMP-2 monomers. A) Formation of disulfide-bonded BMP-2 dimer followed by non-reducing SDS-PAGE analysis and Coomassie Brilliant blue staining. As an example, the analysis of a refolding experiment carried out under standard refolding and dimerization conditions is given. M and D denote the positions of the monomeric and dimeric forms of BMP-2, respectively. On the left-hand side are standards of the purified BMP-2 dimer at the following concentrations: 10, 15, 35, 50 and 80 µg $mL^{-1}$. The samples from the kinetic experiment were concentrated appropriately to allow the quantitative determination of the BMP-2 dimer at different time points of the refolding experiment (2-27 h, 4 X concentrated (4X); 31-46, 2X; 51-60, 1.5X, 65-112, 1X). B) Time depending formation of the disulfide-bonded dimer, obtained from data presented in Figure 1A, given as percentage of the initial concentration of the unfolded and reduced BMP-2 monomer.

## Doc2 - Constraints of the kinetic model

To facilitate the comparison of the folding and association kinetics at different conditions, restrictions were introduced into the basic mathematical model to limit the number of possible solutions.

The basic mathematical model employing one intermediate was as follows:

$\frac{dU}{dt} = -k_u U$ Unfolded and reduced monomer

$\frac{dI}{dt} = k_u U - k_i I$ Intermediate

$\frac{dD}{dt} = 0.5 k_d I$ Correctly folded and dimerized BMP-2

$\frac{dX}{dt} = k_x I$ Unproductive side reaction

Firstly, it was assumed that no other reaction takes place in addition to those above, thus, the rate of decrease of the intermediate equals the rate of formation of X and D:

$k_i = k_x + k_d$

Secondly, as both final productive and unproductive reactions have a common reactant, their kinetic constants can be related by a fraction that corresponds to the final refolding yield:

$k_d = f\, k_i$ and $k_x = (1 - f) k_i$

Factor f can be identified with good accuracy from the mass balance of the initial concentration of the unfolded monomer and the amount of correctly folded BMP-2. However, fitting of the model resulted in several solutions with nearly identical prediction error but different values of the kinetic constants caused by the linear relationships between the model parameters (kinetic constants).

Thirdly, to overcome this problem, a factor (a) was introduced to combine the kinetic constants:

$a = \frac{k_u}{k_i} = \frac{k_u}{k_d} f$

With these restrictions, the following set of mass balances was generated:

$\frac{dU}{dt} = -a\, k_i U$ Equation (1)

$\frac{dI}{dt} = a\, k_i U - f\, k_i\, I - (1 - f) k_i I$ Equation (2)

$\frac{dD}{dt} = 0.5\, f\, k_i I$ Equation (3)

$\frac{dX}{dt} = k_i (1 - f) I$ Equation (4)

This modified model was applied to the data represented in Figure 2C of the main manuscript while varying factor a. Best fitting was obtained for values of factor a between 0.3 and 3.0 or a ratio of $k_u / k_d$, between 0.5 and 5.0, respectively (see Suppl. Figure 2). In this interval the prediction error was minimal and approximately constant. These findings revealed that the rate constants for both reactions on the productive folding pathway are quite similar and at most differ by a factor of 10. However, it cannot be distinguished if the formation of the intermediate or the final formation of the correctly folded and dimerized BMP-2 is rate-determining the productive refolding process.

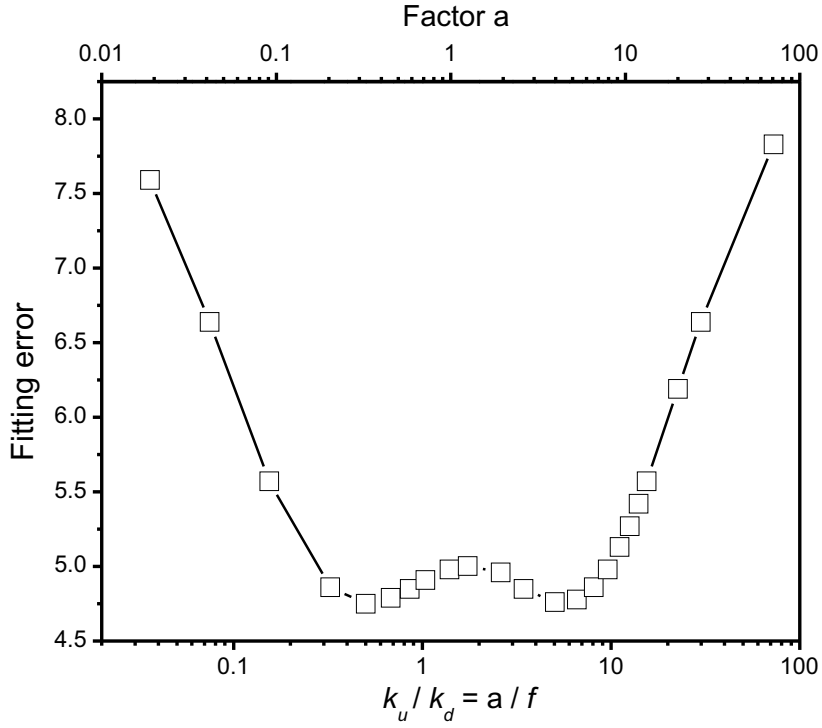


**Suppl Figure 2** Fitting error of the model as a function of factor a. The data shown in Figure 2C of the main manuscript were fitted to the model using different values of a.

To fix the linear relationships between the parameters and to fit the model to the experimental data, a further constraint was introduced. It was assumed that these linear relationships were valid for all experimental conditions and, additionally, factor a was set to a=1. With this constraint (a=1), the kinetic constant of formation of the intermediate is related to the kinetic constant of formation of the final product by a factor equal to the final fraction of dimerization. Likewise, it is related to the kinetic constant of formation of the undesired product by a factor equal to the final fraction of undimerized BMP-2. With this modified model experimental refolding data obtained at all conditions tested were satisfactorily described.